Measurement of the ^{60}Fe$(n, \gamma)^{61}$Fe Cross Section at Stellar Temperatures

E. Uberseder,[1] R. Reifarth,[2] D. Schumann,[3] I. Dillmann,[4,*] C. Domingo Pardo,[4,†] J. Görres,[1] M. Heil,[2] F. Käppeler,[4] J. Marganiec,[4,5,†] J. Neuhausen,[3] M. Pignatari,[6,1] F. Voss,[4] S. Walter,[4] and M. Wiescher[1]

[1]*University of Notre Dame, Department of Physics, Notre Dame, Indiana, USA*
[2]*GSI Darmstadt, Planckstrasse 1, 64291 Darmstadt, Germany*
[3]*Laboratory for Environmental and Radiochemistry, PSI, 5232 Villigen PSI, Switzerland*
[4]*Forschungszentrum Karlsruhe, Institut für Kernphysik, Postfach 3640, D-76021 Karlsruhe, Germany*
[5]*University of Lodz, Poland*
[6]*Keele University, Keele, Staffordshire ST5 5BG, United Kingdom*

(Received 20 August 2008; published 17 April 2009)

Observations of galactic γ-ray activity have challenged the current understanding of nucleosynthesis in massive stars. Recent measurements of ^{60}Fe abundances relative to ^{26}Al^{g} have underscored the need for accurate nuclear information concerning the stellar production of ^{60}Fe. In light of this motivation, a first measurement of the stellar ^{60}Fe$(n, \gamma)^{61}$Fe cross section, the predominant destruction mechanism of ^{60}Fe, has been performed by activation at the Karlsruhe Van de Graaff accelerator. Results show a Maxwellian averaged cross section at $kT = 25$ keV of $9.9 \pm^{2.8(\mathrm{syst})}_{1.4(\mathrm{stat})}$ mbarn, a significant reduction in uncertainty with respect to existing theoretical discrepancies. This result will serve to significantly constrain models of ^{60}Fe nucleosynthesis in massive stars.

DOI: 10.1103/PhysRevLett.102.151101 PACS numbers: 26.20.Np, 25.40.Lw, 27.50.+e, 97.10.Cv

The origin of ^{60}Fe is important for a number of reasons. Its contribution to galactic γ radioactivity provides crucial information for stellar nucleosynthesis [1]. Long-lived γ-ray emitters such as ^{26}Al^{g} and ^{60}Fe are characterized by a diffuse distribution along the galactic plane with the spatial profile of the emission reflecting the galactic distribution of a large number of sources. The isotopes ^{26}Al^{g} and ^{60}Fe are mainly produced in massive stars with $M \geq 8M_{\odot}$ ($M_{\odot}$ stands for the mass of the sun) under both preexplosive and explosive conditions [2–4]. Prior to the supernova explosion, ^{26}Al^{g} is synthesized via proton capture during core or shell H burning and shell C burning, while ^{60}Fe is produced by neutron-capture reactions in the high neutron fluxes reached during shell C burning. The presupernova ^{26}Al^{g} and ^{60}Fe abundances are subsequently modified by the supernova explosion before being ejected into the interstellar medium. Recent ^{60}Fe/^{26}Al^{g} ratios from γ-ray observations with RHESSI (0.097 ± 0.039 [5]) and INTEGRAL (0.11 ± 0.03 [6]) have been confronted by a multitude of massive stars simulations. Apart from the reaction rates associated with the production as well as depletion of ^{26}Al^{g} and ^{60}Fe, the isotopic ratios were found to depend critically on the assumptions for the initial mass function and on the mass loss rate [2,3].

The enrichment in ^{60}Ni in meteoritic inclusions [7–10] indicates that ^{60}Fe has been present in substantial amounts in the early solar system and has been taken as evidence for early injection of ^{60}Fe from a nearby supernova into the protosolar nebula [11–14]. In this way, ^{60}Fe represents an important chronometer for the early solar system (ESS) [15].

The recent discovery of ^{60}Fe in deep sea manganese crusts [16] implies that fresh ^{60}Fe was injected into the solar system 2.8 Myr ago by a nearby supernova when the solar system swept through the expanding SN envelope. The ^{60}Fe/^{56}Fe ratio of 1.9×10^{-15} measured by accelerator mass spectrometry could in principle be used to determine the distance of the SN, an important constraint for the impact of this event on the terrestrial biosphere.

As previously mentioned, a significant contribution to the interstellar ^{60}Fe abundance is provided by the slow neutron-capture (s) process in massive stars. The s process operates in two major evolutionary stages, first during convective core He burning and, subsequently, during convective shell C burning. Neutrons are mainly produced by the ^{22}Ne$(\alpha, n)^{25}$Mg reaction in both cases, but at rather different temperatures and neutron densities [17–19].

As illustrated in Fig. 1, the s-process path to ^{60}Fe, which starts from the most abundant seed nucleus ^{56}Fe, is determined by the branching at ^{59}Fe ($t_{1/2} = 44.5d$). At the low neutron densities during convective core He burning, ^{60}Fe is shielded from the s-process chain, because the β-decay rate of ^{59}Fe dominates over the (n, γ) rate by orders of magnitude. On the other hand, the production of ^{60}Fe

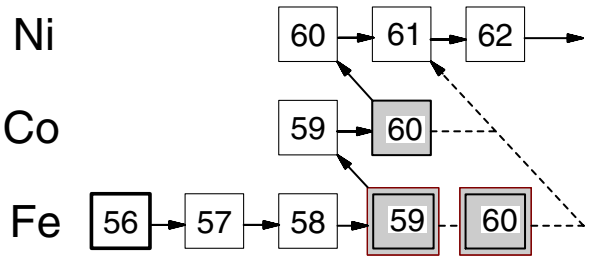

FIG. 1 (color online). The s-process reaction path to ^{60}Fe via the branching at ^{59}Fe.

TABLE I. γ-ray related properties.

Nucleus	E_γ (keV)	ϵ_γ (%)	I_γ (%)	$t_{1/2}$ (min)
^{61}Fe	297.90/1027.42 coinc.	2.59 ± 0.05	22.2 ± 2.9[a]	5.98 ± 0.06[a]
^{61}Fe	1205. 07	8.2 ± 0.1	43.6 ± 4.5[a]	5.98 ± 0.06[a]
^{198}Au	411.80	20.6 ± 0.3	95.58 ± 0.12[b]	3881.0 ± 0.3[b]

[a]Bhat [25].
[b]Chunmei [29].

becomes efficient during the shell C-burning phase, where higher temperatures of $T = (1.0–1.4) \times 10^9$ K give rise to the neutron densities in excess of 10^{11} cm^{-3} necessary for bridging the instability gap at ^{59}Fe.

The interpretation of all the above observations depends critically on the reliability of the stellar models as well as on the neutron-capture rates relevant to the production and depletion of ^{60}Fe [1]. These rates can only be determined reliably in laboratory experiments, because theoretical calculations are too uncertain. Especially in the case of ^{60}Fe, the calculated values may vary by an order of magnitude [20]. In this Letter we present the results of the first experimental study of the ^{60}Fe$(n, \gamma)^{61}$Fe cross section at stellar temperature conditions.

^{60}Fe atoms were extracted from a Cu beam dump previously irradiated with high energy protons at Paul Scherrer Institute, Switzerland. Besides the desired iron isotope, the copper sample contained also about 150 MBq ^{60}Co and 2 MBq ^{44}Ti as the main contaminants. Since the number of ^{60}Fe atoms in the sample had to be determined by the ingrowth of the ^{60}Co activity, these contaminants have been carefully separated by liquid-liquid extraction, resulting in decontamination factors of $\approx 3 \times 10^8$ for ^{60}Co and $\approx 5 \times 10^6$ for ^{44}Ti. Details of the chemical separation can be found in Ref. [21]. In addition to the isotope of interest, the sample contained 100 MBq of ^{55}Fe, which is coproduced along with ^{60}Fe, as well as traces of stable iron isotopes. The ^{60}Fe contained in the final diluted HCl solution was dried on a graphite backing 6 mm in diameter, which served as the sample for the neutron-capture experiment.

The number of ^{60}Fe nuclei was determined from the ingrowth of the daughter activity of ^{60}Co, yielding $(7.8 \pm 1.6) \times 10^{15}$ ^{60}Fe atoms in the sample. This value is uncertain by 20% due to the adopted half-life of ^{60}Fe ($t_{1/2} = 1.5 \pm 0.3$ Myr) [22].

The activation method represents a well established and accurate approach to determine Maxwellian averaged cross sections by producing quasistellar neutron spectra via the ^{7}Li$(p, n)^7$Be reaction [23,24]. In the present experiment, a proton beam with an energy of $E_p = 1912$ keV, 30 keV above the reaction threshold, was delivered by the Karlsruhe 3.7 MV Van de Graaff accelerator with typical intensities of 100 to 150 μA. Under these conditions the neutrons are kinematically collimated into a forward cone of 120° opening angle. Depending on the proton beam current and the performance of the ^{7}Li targets, a neutron source strength of $(2 - 4) \times 10^9$ s^{-1} was obtained. Throughout the irradiations the neutron flux was continuously monitored and recorded in time steps of 10 s by means of a ^{6}Li-glass detector located 1 m downstream of the target.

Because of the short half-life of ^{61}Fe ($t_{1/2} = 5.98 \pm 0.06$ min [25]), the experiment was divided into 47 repeated irradiations. The irradiations lasted for 15 min, followed by a transfer time of about 60 s from the irradiation position to the counting station, where the activity was measured for 10 min. The subsequent irradiation was then started after an additional waiting time of about 15 min. The ^{60}Fe sample was sandwiched between 0.03 mm thick gold foils used in the determination of the time-integrated neutron flux. The energy dependent gold cross section of Macklin [26] was matched to new low energy data from the n_TOF collaboration [27] and normalized to the accurate result of the activation measurement by Ratynski and Käppeler [28].

The induced activities are characterized by γ-ray lines with known absolute intensities (Table I) [25,29] and were counted with a pair of HPGe clover detectors, each with a relative efficiency of 120%. By arranging the detectors face to face in very close geometry, absolute peak efficiencies of 26% and 10% could be achieved at 298 and 1027 keV, respectively. The positions of the detectors and of the sample were exactly defined by a special sample holder to ensure that the counting geometry was reproducible within ±0.1 mm. The detectors were shielded against ambient background by 10 cm of lead and by an inner layer of 5 mm copper.

The intrinsic γ-ray background presented a serious problem for the activity measurements. At low energies, the γ spectrum was dominated by internal bremsstrahlung from the decay of the ^{55}Fe impurity, thus impeding the 298 keV line expected to show the best signature for the decay of ^{61}Fe. At higher energies, the detection of the stronger lines at 1027 and 1205 keV was limited by the lower detection efficiency and natural background. This problem could be overcome by making use of the eightfold segmentation of the Ge clover array [30]. Requiring coincidence detection of the 298/1027 keV cascade transitions provided excellent sensitivity. Figure 2 shows that a nearly background free spectrum could be obtained in this way, although with reduced counting statistics. The 1205 keV line could also be included in the analysis after the background was reduced by means of multiplicity cuts.

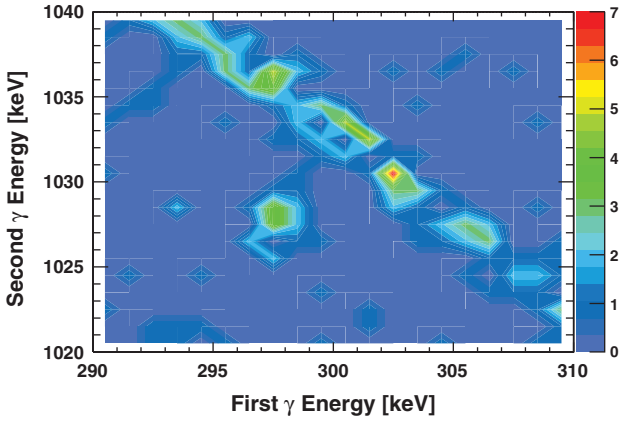

FIG. 2 (color). Coincidence spectra of the 298–1027 keV cascades in the decay of ^{61}Fe. The diagonal feature corresponds to events with multiplicity two originating from scattering of the 1332 keV ^{60}Co line.

The number of activated nuclei per cycle, A_n, is

$$A_n = \phi_n \cdot N \cdot \sigma \cdot f_b^n, \tag{1}$$

where ϕ is the time-integrated neutron flux, N the number of sample atoms, and σ the spectrum averaged neutron-capture cross section. The factor f_b accounts for variations of the neutron flux and for the decay during activation. Using Eq. (1), the total number of counts in a characteristic γ-ray line is

$$C_\gamma = N\sigma K_\gamma \varepsilon_\gamma I_\gamma [1 - \exp(-\lambda t_m)] \sum_n f_b^n \phi_n \exp(-\lambda t_w^n), \tag{2}$$

where K_γ is a correction factor for γ-ray self-absorption, summing, and extended source effects; ε_γ the detection efficiency of the HPGe clover array; I_γ the line intensity; λ the decay rate of ^{61}Fe; t_w^n the waiting time between irradiation and counting; and t_m the duration of the activity measurement. The time-integrated flux per activation, ϕ_n, is determined from the measured intensities of the 412 keV γ-ray line in the spectra of the two gold foils.

To determine the correction factor, K_γ, GEANT4 [31] simulations were performed using the RadioactiveDecay3.1 database with a careful modeling of the detector geometry. In addition, corrections to the detector efficiency for the multiplicity cuts were also simulated. These corrections are of the order of 4% to 18%.

After summing up the results of all 47 activations, one obtains an average experimental cross section of $10.2 \pm {}^{2.9(\mathrm{syst})}_{1.4(\mathrm{stat})}$ mbarn. The experimental error is dominated by the uncertainties of the counting statistics (12%–15%) and the ^{60}Fe determination (25%). The experimentally derived cross section is particularly sensitive to the half-life of ^{60}Fe used to determine the number of ^{60}Fe atoms. A new, more accurate half-life would result in an improved cross section $\sigma_{\mathrm{new}} = 10.2 \times (1.5\ \mathrm{Myr}/t_{1/2})$.

The final Maxwellian averaged cross sections listed in Table II

$$\frac{\langle \sigma v \rangle}{v_T} = \frac{2}{\sqrt{\pi}} \frac{\int_0^\infty \sigma(E_n) E_n \exp(-E_n/kT) dE_n}{\int_0^\infty E_n \exp(-E_n/kT) dE_n} \tag{3}$$

are obtained by folding the energy differential (n, γ) cross section, $\sigma_{n,\gamma}(E_n)$, calculated using the Hauser-Feshbach statistical model [20] with the experimental neutron energy distribution to obtain a normalization factor, which is applied to the energy differential cross section. This normalized $\sigma_{n,\gamma}(E_n)$ is then folded with a true Maxwell-Boltzmann distribution at temperatures of astrophysical interest. Such a procedure corrects for the slight discrepancies between the experimental neutron distribution and a true Maxwell-Boltzmann distribution at kT = 25 keV.

The energy dependence of the cross sections has a marginal effect on the results at kT = 25 keV, because this thermal distribution is almost perfectly simulated by the experimental neutron spectrum. However, it becomes a crucial problem for the extrapolation towards lower and higher thermal energies, particularly since the pronounced resonance structure expected for the cross section of ^{60}Fe is not described by this model. Comparison with similar cases in this mass region shows that extrapolation uncertainties may grow up to about 20% at kT = 90 keV, the thermal energy during shell C burning in massive stars [24].

The effect of the nuclear physics uncertainties on the neutron-capture nucleosynthesis of ^{60}Fe has been investigated using model calculations for a $25M_\odot$ star. As these results refer only to a single stellar mass, they can obviously not be used to constrain the galactic production of ^{60}Fe. While this aspect is discussed, for example, in Ref. [3], the present study is intended to illustrate the sensitivity to the nuclear input data. In Fig. 3, the ^{60}Fe abundances are given in terms of mass fraction at the end of shell C burning and before the supernova, since the C-shell phase contributes significantly to the total production of ^{60}Fe. The horizontal line indicates the situation obtained with the adopted rates for the (n, γ) cross sections of ^{58}Fe [24], ^{59}Fe [20], and ^{60}Fe (this work) as well as for the stellar β-decay rates of ^{59,60}Fe [33]. The open circles represent the results found by variation of the adopted rates by factors of 0.5 and 2, corresponding to plausible estimates of the respective uncertainties.

In the case of the (n, γ) cross section of ^{60}Fe, the remaining uncertainty is shown by the error bars of the

TABLE II. Maxwellian averaged cross sections (in mbarn) of ^{60}Fe$(n, \gamma)^{61}$Fe for kT = 25–100 keV.

kT	25	30	40	60	80	100
This work	**9.9** $\pm {}^{2.8(\mathrm{syst})}_{1.4(\mathrm{stat})}$	9.0	7.8	6.2	5.3	4.7
Ref. [32]	4.1	3.9	3.4	2.6	2.2	1.9
Ref. [20]	5.9	5.3	4.6	3.6	3.1	2.7

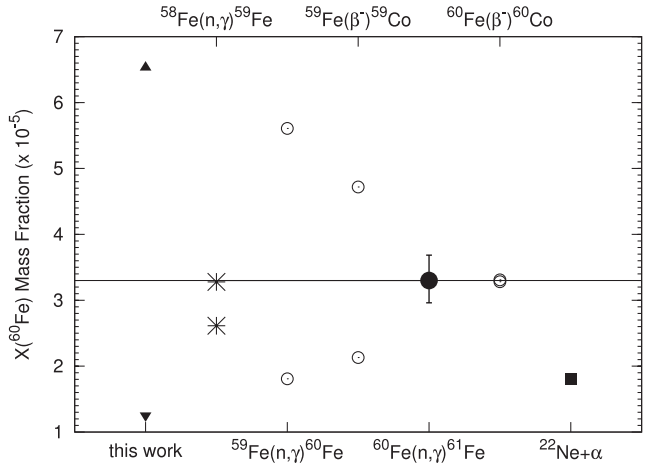

FIG. 3. The sensitivity of the ^{60}Fe production to variation of the main nuclear physics data. The respective reactions and decays are specified below and above the figure. The improvement by the present result is indicated by the error bars of the solid black circle. For more details, see the text.

solid black circle. Since this uncertainty can be further reduced by a more accurate ^{60}Fe half-life, the ^{60}Fe cross section is now of minor importance for the ^{60}Fe problem. The same holds for the ^{58}Fe cross section (stars in Fig. 3), for which a fairly accurate value has been recently reported [24]. In this case, the asymmetric variation of ^{60}Fe corresponds to the upper and lower bounds of the quoted cross section. The remaining uncertainties in the nuclear input are dominated by the branching point at ^{59}Fe. A similar sensitivity is observed with respect to the $^{22}\mathrm{Ne} + \alpha$ reaction. The black square was obtained by replacing the adopted rates for $^{22}\mathrm{Ne}(\alpha, n)$ [34] and $^{22}\mathrm{Ne}(\alpha, \gamma)$ [35] by the values of the NACRE compilation [36]. All of these remaining problems represent enormous experimental challenges, which can be met only with future facilities.

Apart from the nuclear input, the stellar models are still subject to large uncertainties. For example, a 5% change of the temperature during shell C burning affects the maximum neutron density, resulting in a variation of the pre-explosive production of ^{60}Fe, as indicated by the black triangles in Fig. 3. Further uncertainties are related to the explosive nucleosynthesis of ^{60}Fe by the supernova. A reliable basis of the relevant nuclear physics data would contribute significantly to further studies of the stellar production of ^{60}Fe.

We would like to thank S. Köchli and S. Horn for performing the chemical and radiochemical analyses. M. P. is supported by a Marie Curie International Reintegration Grant MIRG-CT-2006-046520 within the European FP6, and by NSF Grant No. PHY 02-16783 (JINA).

*Present address: Physik-Department E12, Technische Universität München, Garching, Germany.
†Present address: GSI Darmstadt, Planckstrasse 1, 64291 Darmstadt, Germany.

[1] R. Diehl, N. Prantzos, and P. von Ballmoos, Nucl. Phys. **A777**, 70 (2006).
[2] F. Timmes *et al.*, Astrophys. J. **449**, 204 (1995).
[3] M. Limongi and A. Chieffi, Astrophys. J. **647**, 483 (2006).
[4] S. E. Woosley and A. Heger, Phys. Rep. **442**, 269 (2007).
[5] D. Smith, arXiv:astro-ph/0404594v1.
[6] M. Harris *et al.*, Astron. Astrophys. **433**, L49 (2005).
[7] J. Birck and G. Lugmair, Earth Planet. Sci. Lett. **90**, 131 (1988).
[8] G. Quitté *et al.*, Astrophys. J. **655**, 678 (2007).
[9] Y. Guan, G. Huss, and L. Leshin, Geochim. Cosmochim. Acta **71**, 4082 (2007).
[10] F. Moynier *et al.*, Geochim. Cosmochim. Acta **71**, 4365 (2007).
[11] S. Mostefaoui, G. Lugmair, and P. Hoppe, Astrophys. J. **625**, 271 (2005).
[12] L. Looney, J. Tobin, and B. Fields, Astrophys. J. **652**, 1755 (2006).
[13] N. Dauphas *et al.*, Astrophys. J. **686**, 560 (2008).
[14] N. Ouellette, S. Desch, and J. Hester, Astrophys. J. **662**, 1268 (2007).
[15] A. Boss, Astrophys. J. **660**, 1707 (2007).
[16] K. Knie *et al.*, Phys. Rev. Lett. **93**, 171103 (2004).
[17] C. Raiteri, M. Busso, R. Gallino, and G. Picchio, Astrophys. J. **371**, 665 (1991).
[18] C. Raiteri *et al.*, Astrophys. J. **419**, 207 (1993).
[19] M. Limongi, O. Straniero, and A. Chieffi, Astrophys. J. Suppl. Ser. **129**, 625 (2000).
[20] T. Rauscher and F.-K. Thielemann, At. Data Nucl. Data Tables **75**, 1 (2000).
[21] D. Schumann and J. Neuhausen, J. Phys. G **35**, 014 046 (2008).
[22] J. Tuli, Nuclear Data Sheets **100**, 347 (2003).
[23] H. Beer and F. Käppeler, Phys. Rev. C **21**, 534 (1980).
[24] M. Heil *et al.*, Phys. Rev. C **77**, 015808 (2008).
[25] M. Bhat, Nuclear Data Sheets **88**, 417 (1999).
[26] R. Macklin (private communication to National Nuclear Data Center). See also www.nndc.bnl.gov/exfor, accession number 12720.
[27] C. Massimi *et al.*, Proc. Sci., NIC X 080 (2008).
[28] W. Ratynski and F. Käppeler, Phys. Rev. C **37**, 595 (1988).
[29] Z. Chunmei, Nuclear Data Sheets **95**, 59 (2002).
[30] R. Reifarth *et al.*, Astrophys. J. **582**, 1251 (2003).
[31] J. Allison *et al.*, IEEE Trans. Nucl. Sci. **53**, 270 (2006). See also http://cern.ch/geant4/.
[32] S. E. Woosley, W. A. Fowler, J. A. Holmes, and B. A. Zimmerman, At. Data Nucl. Data Tables **22**, 371 (1978).
[33] K. Takahashi and K. Yokoi, At. Data Nucl. Data Tables **36**, 375 (1987).
[34] M. Jaeger *et al.*, Phys. Rev. Lett. **87**, 202501 (2001).
[35] M. Pignatari, Ph.D. thesis, University of Torino, 2006.
[36] C. Angulo *et al.*, Nucl. Phys. **A656**, 3 (1999).